IIETA International Information and Engineering Technology Association
Advancing the World of Information and Engineering

Revue des Composites et des Matériaux Avancés-Journal of Composite and Advanced Materials
Vol. 35, No. 5, October, 2025, pp. 893-900
Journal homepage: http://iieta.org/journals/rcma

Nonlinear Thermal Effects on Cylindrical Bending of Orthotropic Plate: A Computational Study

Sanjay Kantrao Kulkarni

Department of Civil Engineering, Symbiosis Institute of Technology (SIT), Symbiosis International (Deemed University), Pune 412115, India

Corresponding Author Email: sanjay.kulkarni@sitpune.edu.in

https://doi.org/10.18280/rcma.350509

Received: 3 September 2025
Revised: 3 October 2025
Accepted: 26 October 2025
Available online: 31 October 2025

Keywords:
thermal analysis, thermal deformations, nonlinear thermal load, higher order theory, cylindrical bending

ABSTRACT

Orthotropic plates are used in advanced structures where directional stiffness is critical. Under nonlinear thermal loading their bending behaviour becomes complex and demands advanced modelling techniques. The primary goal of this study is to formulate and validate a numerical approach for evaluating the thermally induced cylindrical bending of orthotropic plate under nonlinear temperature distribution. The study investigates the influence of nonlinear thermal loading on the cylindrical bending behaviour of the orthotropic plate. The applied thermal profile comprises a base temperature field, a linear gradient across plate's thickness and an additional nonlinear or complex variation along the same dimension. Such a composite temperature distribution is essential for capturing the realistic thermal response of orthotropic laminated structures subjected to cylindrical bending. To analyse the resulting thermal deformations a higher order trigonometric plate theory is employed under both linear and nonlinear thermal conditions. For comparative evaluation, a parabolic plate theory is also utilized, specifically to assess the accuracy and performance of the trigonometric model when exposed to nonlinear or complex thermal gradients. The mathematical model is derived using energy principles and solved analytically via Navier's type series expansion. A simulation tool is developed in FORTRAN to analyse the thermal stresses and deflections under nonlinear thermal loadings. Simulation results demonstrate that a nonlinear thermal load intensify the results of axial and transverse displacements. The developed analytical framework effectively captures the nonlinear thermal effects in orthotropic plate undergoing cylindrical bending.

1. INTRODUCTION

The cylindrical bending idealization treats a laminated plate as infinitely long in one direction and simply supported along its edges, enabling a clean separation of variables for studying flexure under mechanical or thermal fields. Modern plate and elasticity theories have significantly sharpened our understanding of how composite laminates respond in such one-dimensional bending states, especially when the temperature field is nonuniform and the coupling is nonlinear. Building on earlier nth-order and higher-order formulations applied to orthotropic laminates and sandwich constructions [1-3], as well as exact three-dimensional and discrete-layer solutions that exposed the limits of classical plate theory (CPT) [4, 5], subsequent work has spanned dynamic behavior, piezoelectric coupling, and refined shear/normal-deformation kinematics in cylindrical bending [6-18].

In the last few years, several trends stand out. First, a notable advancement in the field is the refinement of semi-analytical and isogeometric scaled boundary finite element methods. These techniques have proven highly effective for analyzing cylindrical bending in thick, layered composite structures, offering excellent precision while maintaining computational efficiency number of through a reduced number of degrees of freedom [19-25]. Second, realistic service conditions—moisture diffusion, temperature gradients, and elastic foundations—are now embedded directly in cylindrical-panel models; for example, quasi-static hygrothermal bending of laminated cylindrical panels has been analyzed with fully coupled field equations [20]. Third, thermal boundary complexities are being resolved explicitly: laminated plates with arbitrary edge restraints subjected to non-uniform temperature fields admit efficient analytical–numerical solutions that are immediately useful for validation and benchmarking [21]. Fourth, data-assisted and energy-variational solvers are being used to capture geometric nonlinearity in laminated plates with high fidelity, pointing to robust surrogates for demanding bending cases [22]. Fifth, coupled thermo-mechanical analyses for advanced constituents—such as graphene-reinforced functionally graded plates—now quantify post-buckling and large-deflection responses under prescribed temperature fields, informing design under severe environments [23-28]. The study of material orthotropy and length to thickness ratio on

transverse displacement of sandwich beam was studied and presented by Kulkarni [29] using parabolic shear deformation theory (PSDT).

Against this backdrop, the analysis of an orthotropic plate strip under a nonlinear through-thickness temperature profile in cylindrical bending remains comparatively under-reported. The present study addresses that gap by quantifying how a nonlinear thermal field modifies the stress resultants and interlaminar stress distributions of an orthotropic plate subjected to cylindrical bending.

2. METHODOLOGY

The following Figure 1 illustrates an orthotropic plate strip with its coordinate system. The strip extends significantly in the *y* direction, while its length in the *x* direction is limited and denoted by "*a*". The *z* axis points downward through the thickness of the plate strip.

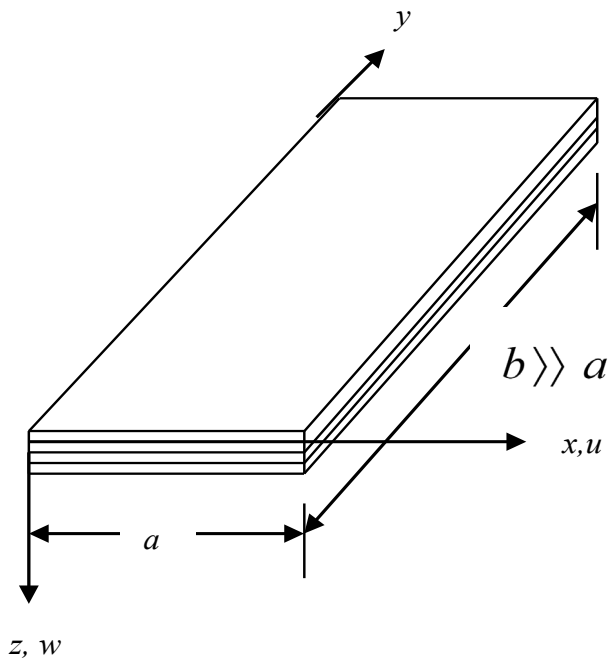

Figure 1. A coordinate system of an orthotropic plate strip

In structural mechanics, higher order theories play a vital role in the analysis of plates that experience a significant shear effect under nonlinear thermal load. In present case higher order trigonometric and Parabolic plate theories are used to understand the effect of nonlinear thermal load on orthotropic plate in cylindrical bending. The displacement field of trigonometric plate theory is represented by the following Eqs. (1) and (2). Trigonometric and parabolic plate theories describe how plates deform due to shear forces. These are known as shear deformation theories. From this point forward, these theories are referred to as Trigonometric Shear Deformation Theory (TSDT) and PSD.

$$u(x,z) = -z\frac{\partial w(x)}{\partial x} + \frac{h}{\pi}\sin\frac{\pi z}{h}\varphi(x) \tag{1}$$

$$w(x) = w(x) \tag{2}$$

In the referenced expression (1) and (2), the variable *u* denotes displacement along the axial (*x* axis), whereas *w* represents displacement in transverse direction (*z* axis). The function ∅ in Eq. (1) is unknown rotation to be determined. The strains are evaluated with reference to elasticity theory as given by following Eq. (3).

$$\varepsilon_x = \frac{\partial u}{\partial x}, \gamma_{zx} = \frac{\partial u}{\partial z} + \frac{\partial w}{\partial x} \tag{3}$$

The relationship between stress and strain for an orthotropic plate strip is represented by below Eq. (4).

$$\begin{Bmatrix} \sigma_x \\ \tau_{zx} \end{Bmatrix} = \begin{bmatrix} \bar{Q}_{11} & 0 \\ 0 & \bar{Q}_{55} \end{bmatrix} \begin{Bmatrix} \varepsilon_x - \alpha_x T \\ \gamma_{zx} \end{Bmatrix} \tag{4}$$

The reduced stiffness coefficients are represented by $\bar{Q}_{ij}$ in Eq. (4) are defined in Eq. (5).

$$\bar{Q}_{11} = Q_{11} = \frac{E_1}{1-\mu_{12}\mu_{21}}, \bar{Q}_{55} = Q_{55} = G_{13} \tag{5}$$

In the above Eq. (5), the parameters are defined as follows: E represents the modulus of elasticity, μ denotes Poisson's ratio, G is the shear modulus, α_x indicates the coefficient of thermal expansion along the *x* axis and *T* corresponds to the change in temperature. Furthermore, Eq. (6) describes the temperature distribution within the system, where the temperature at any specific location is a function of both the horizontal coordinate (*x*) and the vertical coordinate (*z*), expressed as *T* (*x, z*).

$$T(x,z) = T_1(x) + \frac{z}{h}T_2(x) + \frac{\psi(z) = \frac{h}{\pi}\sin\frac{\pi z}{h}}{h}T_3(x) \tag{6}$$

The above Eq. (6) characterizes how temperature varies along the depth of the beam structure. This thermal profile is influenced by three disctinct thermal loads, denoted as T_1, T_2 and T_3. Among these the component T_2 contrubutes to a linearly varying temperature field, reflecting a uniform thermal gradient across the beam's thickness. In contrast, the influence of T_3 introduces a nonlinear variation mathematically described by the function $\left(\psi(z) = \frac{h}{\pi} sin\frac{\pi z}{h}\right)$, where, h is the total depth of the beam and z is vertical coordinate. This sinusoidal term captures the oscillatory nature of the temperature distribution induced by T_3, offering a more complex thermal behaviour compared to the linear case. In this analysis, the thermal load applied follows a sinusoidal pattern.

2.1 Equations of motion

The equations of motion are derived using the principle of virtual work, which asserts that for a system subjected to infinitesimal virtual displacements, the external work performed must be exactly balanced by the internal work generated by the system's internal forces. This principle forms the foundation of the variational approach, a powerful technique for formulating the governing differential equations of structural behaviour. Once these equations are established, Navier's method employed to compute the resulting displacements and stress fields under thermal loadings. By

applying this principle to an orthotropic plate strip, one can derive the corresponding governing equations or equation of motion that describe its mechanical behaviour. The following Eq. (7) represents an application of the virtual work principle to an orthotropic plate in cylindrical bending.

$$\int_{-\frac{h}{2}}^{\frac{h}{2}}\int_0^a (\sigma_x \delta\varepsilon_x + \tau_{zx}\delta\gamma_{zx})dxdz = 0 \tag{7}$$

To solve the above Eq. (7), the method of integration by parts is employed, which facilitates the transformation of the variational expression into a more tractable form. This mathematical technique allows the redistribution of derivatives between functions ultimately leading to the derivation of the systems' governing equations. As a result of this process, the fundamental equations of motion are obtained and these are represented by the following Eqs. (8) and (9).

$$\begin{aligned}&\delta w : Q_{11}\frac{h^3}{12}\frac{\partial^4 w}{\partial x^4} - Q_{11}\frac{2h^3}{\pi^3}\frac{\partial^3 \varphi}{\partial x^3} \\ &+\alpha_x Q_{11}\frac{h^2}{12}\frac{\partial^2 T_1}{\partial x^2} + \alpha_x Q_{11}\frac{2h^2}{\pi^3}\frac{\partial^2 T_3}{\partial x^2} = 0\end{aligned} \tag{8}$$

$$\begin{aligned}&\delta\varphi : Q_{11}\frac{2h^3}{\pi^3}\frac{\partial^3 w}{\partial x^3} - Q_{11}\frac{h^3}{2\pi^2}\frac{\partial^2 \varphi}{\partial x^2} + Q_{55}\frac{h}{2}\varphi \\ &+\alpha_x Q_{11}\frac{2h^2}{\pi^3}\frac{\partial T_2}{\partial x} + \alpha_x Q_{11}\frac{h^2}{2\pi^2}\frac{\partial T_3}{\partial x} = 0\end{aligned} \tag{9}$$

2.2 Material properties

The material properties used in the analysis are given in Eq. (10) below.

$$\frac{E_1}{E_2} = 25, G_{12} = G_{13} = 0.5E_2, \mu_{12} = 0.25, \frac{\alpha_2}{\alpha_1} = 3 \tag{10}$$

The moderate modular ratio and low ratio of thermal expansion coefficients is considered for analysis. E_1 and E_2 represent Young's modulus in fibre (1) and transverse (2) directions are shown in Figure 2. A ratio of 25 indicates the material is highly stiff along the fibre axis compared to the transverse direction. This is typically a fibre reinforced composite where fibres dominate stiffeness in one direction. Such anisotropy is very crucial in applications demanding directional strength, like aerospace panels.

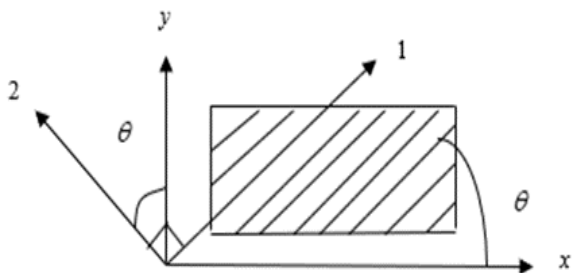

Figure 2. Orientation of fibre and transverse directions

The shear modulus is denoted by G_{12} and G_{13} in the planes involving the fibre direction. Setting these shear moduli to half of E_2 indicates moderate resistance to shear deformation especially in the directions involving the weaker transverse axis. This balance helps to ensure the material can tolerate torsional load without being over rigid. This helps to prevent cracking under complex stresses. The value of Poisson's ratio indicates that when the material is stretched along fibre direction, it contracts 25% as much in the transverse direction. The symbols α_1 and α_2 indicate how much a material streaches with heat along and across the fibre directions, respectively. A ratio of coefficient of thermal expansion of 3 implies that the material expands 3 times more in transverse direction (2) than along the fibre direction (1) or axis when heated. The low coefficient of thermal expansion minimizes warping in the structural member.

2.3 Navier's solution

The Navier's solution technique is an analytical approach used to solve problems in elasticity and plate theory. It is especially useful in thermal stress analysis where temperature stresses are induced under simply supported boundary conditions. This method is very effective in scenarios which involves temperature variations, where uneven heating leads to internal stresses and structural distortion. By expressing displacement and stress components as series expansions, Navier's technique simplifies the complex equations governing plate deformation under thermal influence. The solution fulfills the conditions as given in the below Eq. (11).

$$w = 0, M_x = 0, N_x = 0, M_x^s = 0 \tag{11}$$

In the above equation, the term w is the transverse displacement which is zero; this implies the simply supported boundary conditions. The term M_x is bending moment in x direction has a value of zero, indicating that no resistance to bending since simply supported edge. The term N_x is in-plane normal force in x direction and has the value zero. This indicates no axial force along x direction at the boundary. This is important in thermal stress analysis where expansion or contraction may occur.

The unknowns given below are represented in trigonometric form which satisfy the exact boundary conditions. Thermal load expansion is expressed using a single sine term from the Fourier series, as illustrated below in the Eqs. (12) to (16).

$$w(x) = \sum_{m=1}^{\infty} w_m \sin\frac{m\pi x}{a} \tag{12}$$

$$\varphi(x) = \sum_{m=1}^{\infty} \varphi_m \cos\frac{m\pi x}{a} \tag{13}$$

$$T_1(x) = \sum_{m=1}^{\infty} T_{1m} \sin\frac{m\pi x}{a} \tag{14}$$

$$T_2(x) = \sum_{m=1}^{\infty} T_{2m} \sin\frac{m\pi x}{a} \tag{15}$$

$$T_3(x) = \sum_{m=1}^{\infty} T_{3m} \sin\frac{m\pi x}{a} \tag{16}$$

The first harmonic of a Fourier sine series or first mode of sinusoidal thermal distribution is represented by $T_{1m} = T_{2m} = T_{3m} = T_1 = T_2 = T_3,\ m = 1$. This implies that only the first

term in the series is active representing a single sinusoidal wave across the thickness in one direction.

Substitution of the solution into the equations of motion results into a set of algebraic equations. This can be represented by following Eq. (17).

$$[K]\{\delta\} = \{f\} \tag{17}$$

The symmetric stiffness is represented by [*K*]. The coefficients of the stiffness matrix [*K*] are as given in the following Eq. (18).

$$\begin{bmatrix} K_{11} & K_{12} \\ K_{21} & K_{22} \end{bmatrix} = \begin{bmatrix} D_1 \dfrac{m^4\pi^4}{a^4} & -D_4 \dfrac{m^3\pi^3}{a^3} \\ -D_4 \dfrac{m^3\pi^3}{a^3} & D_9 \dfrac{m^2\pi^2}{a^2} + D_{11} \end{bmatrix} \tag{18}$$

The $\{\delta\}$ in Eq. (17) is given by the following Eq. (19).

$$\{\delta\} = \{w_m, \varphi_m\} \tag{19}$$

The force vector is denoted by $\{f\}$ in the above Eq. (17). The elements of the thermal load vector $\{f\}$ are given below Eq. (20).

$$\begin{Bmatrix} f_1 \\ f_2 \end{Bmatrix} = \begin{Bmatrix} R_1 \dfrac{m^2\pi^2}{a^2} T_{2m} + R_2 \dfrac{m^2\pi^2}{a^3} T_{3m} \\ -R_5 \dfrac{m\pi}{a} T_{2m} - R_6 \dfrac{m\pi}{a} T_{3m} \end{Bmatrix} \tag{20}$$

By solving this system of equation, it becomes possible to determine the values represented by $\{\delta\}$, which in turn allows for the calculation of stresses and resulting displacements within the structure.

3. RESULTS AND DISCUSSION

Thermal deformation behaviour has been analysed using four distinct plate theories: higher order trigonometric (TSDT), PSDT first order shear deformation (FSDT) and CPT. These models are applied to orthotropic plate undergoing cylindrical bending under linear and nonlinear thermal loading conditions. The calculations are performed for aspect ratios of 4 and 10. The aspect ratio (*a/h*) is denoted by *S* in the result tables. To ensure consistency and clarity all stress and displacement outcomes are presented in the normalized form in Eqs. (21)-(24).

$$\bar{u}\left(0, -\frac{h}{2}\right) = \frac{u}{\alpha_1 T_0 a^2} \tag{21}$$

$$\bar{w}\left(\frac{a}{2}, 0\right) = \frac{10 \times h \times w}{\alpha_1 T_0 a^2} \tag{22}$$

$$\bar{\sigma}_x\left(\frac{a}{2}, -\frac{h}{2}\right) = \frac{\sigma_x}{E_2 \alpha_1 T_0 a^2} \tag{23}$$

$$\bar{\tau}_{zx}^{EE}(0,0) = \frac{\tau_{zx}}{E_2 \alpha_1 T_0 a^2} \tag{24}$$

The transverse shear stresses are critical under nonlinear thermal loading. To capture the exact thermal behaviour of these stresses, equation of equilibrium is used and given as below Eq. (25).

$$\tau_{zx} = -\cdot \int_{z=-\frac{h}{2}}^{+\frac{h}{2}} \frac{\partial \sigma_x}{\partial x} \cdot dz + C \tag{25}$$

In the above equation the constant of integration "*C*" is calculated by using boundary conditions and upon substitution in the Eq. (25), shear stress can be calculated. In the above Eq. (25) the term (τ_{zx}) represents the shear force per unit area acting along *x* axis on a surface normal to the *z* axis. The term (σ_x) is normal stress in the *x* direction and varies due to temperature gradients. The term $\left(\frac{\partial \sigma_x}{\partial x}\right)$ in the above Eq. (25) represents spatial derivative of normal stress which captures how the normal stress changes along the length. Since these stresses vary through the thickness under thermal loading, integrating across the thickness of the plate from bottom (*h/2*) to top (*-h/2*) captures the cumulative effect of these variations across the total depth (*h*). Figure 3 illustrates the upper and lower surfaces of the plate undergoing cylindrical bending.

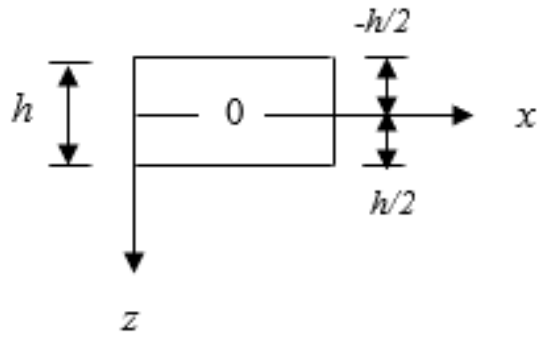

Figure 3. The cross section of plate in cylindrical bending

The integration constant accounts for boundary conditions and ensure the solution satisfies equilibrium. The above Eq. (25) says that to maintain equilibrium under thermal loading, the transverse shear stress must balance the gradient of normal stress through the thickness.

The results of thermal deformations in dimensionless form under linear (L) and nonlinear (NL) thermal loadings are presented in Tables 1 and 2 below. For linear (L) thermal load $T_2 = 1$ and $T_1 = T_3 = 0$. In case of nonlinear (NL) thermal load the thermal loads are $T_1 = 0$ and $T_2 = T_3 = 1$. The importance of Tables 1 and 2 is that both tables show how temperature variations affect displacements and stresses under linear and nonlinear thermal loads.

In linear thermal load case (L), all theories give identical results of axial displacements for an aspect ratio 4 and 10. This implies that axial displacement does not get affected under linear thermal load. In case of nonlinear load (NL), higher theories TSDT and PSDT predicts higher values of axial displacements. Nonlinearity in thermal load increases axial displacement. First order and classical do not provide results under nonlinear thermal load. There is no significant variation in the results of transverse displacement evaluated by all theories for an aspect ratio 4 and 10 under linear thermal load (L). However, nonlinear thermal loading (NL) greatly amplifies transverse displacements for thick and thin orthotropic plate under cylindrical bending. Aspect ratio has

negligible effect on axial displacements. The percentage difference between the values of axial and transverse displacements under linear and nonlinear thermal load is 55% as shown in Table 1. The nonlinear thermal loading leads to large temperature gradients through the thickness. These gradients include higher thermal strains which ultimately amplify the bending and stretching of the plate under cylindrical bending. As temperature increases nonlinearity, the material expands more aggressively this causes significant deformation which linear model fails to capture. The 55% rise in displacements is a direct result of this intensified thermal expansion. In linear model, temperature is assumed to vary mildly. But in reality, nonlinear profiles cause uneven stress distribution leading to larger deflections. Higher order theories like TSDT and PSDT include higher order terms in the displacement field. These terms allow the model to account for shear deformation and thickness wise variation in strain. Thus, the higher order theories are essential to capture realistic stress and displacement analysis in advanced materials. Whereas FSDT and CPT do not show nonlinear results since they lack necessary terms to capture these effects.

Table 1. Normalized displacements values for an orthotropic plate under cylindrical bending influenced by linear (L) and nonlinear thermal (NL) loads with aspect ratios 4 and 10

Theory		$\bar{u}$			$\bar{w}$		
	S	L	NL	% Difference	L	NL	% Difference
TSDT	4	0.1592	0.2814	55.46	1.0132	1.7635	54.04
PSDT		0.1595	0.2828	55.76	1.0238	1.8126	55.61
FSDT		0.1592	-	-	1.0132	-	-
CPT		0.1592	-	-	1.0132	-	-
TSDT	10	0.1592	0.2822	55.73	1.0132	1.7918	55.55
PSDT		0.1594	0.2829	55.84	1.0200	1.8071	55.68
FSDT		0.1592	-	-	1.0132	-	-
CPT		0.1592	-	-	1.0132	-	-

Table 2. Normalized stress values for an orthotropic plate under cylindrical bending influenced by linear (L) and nonlinear thermal (NL) loads with aspect ratios 4 and 10

Theory		$\bar{\sigma}_x$		$\bar{\tau}_{zx}^{EE}$		
	S	L	NL	L	NL	Remark
TSDT	4	0.0003	-1.6426	0.0000	-0.0859	Values are less than zero
PSDT		-0.0267	-1.7601	-0.0004	-0.0904	Values are less than zero
FSDT		0.0000	-	0.0000	-	-
CPT		0.0000	-	0.0000	-	-
TSDT	10	0.0001	-1.7053	0.0000	-0.0357	Values are less than zero
PSDT		-0.0171	-1.7463	-0.0001	-0.0361	Values are less than zero
FSDT		0.0000	-	0.0000	-	-
CPT		0.0000	-	0.0000	-	-

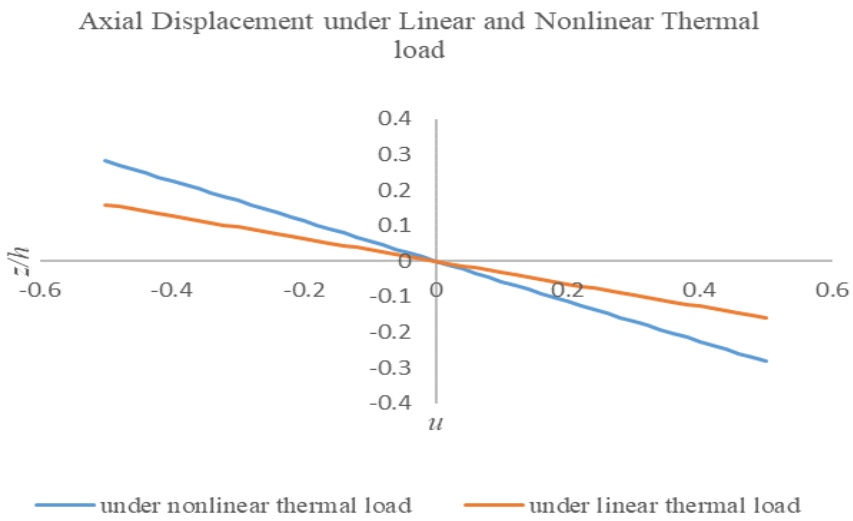

Figure 4. Variation of axial displacement ($\bar{u}$) through the thickness (h) under linear and nonlinear thermal load for an aspect ratio 4

The results of normal stresses are very small under linear thermal load (L) and nonlinear thermal load (NL). Nonlinearity in thermal load does not affect normal stress significantly. The transverse shear stresses are affected strongly than normal stresses by the influence of aspect ratio. Slender plate in cylindrical bending experiences reduced shear

stresses under nonlinear thermal load (NL). The results of transverse shear stresses appear to be highly sensitive to the choice of theory. It is noted that nonlinear thermal effects reduce shear stresses as the plate becomes thinner. Aspect ratio plays an important role under nonlinear thermal load, where slender plate relieves thermal shear stress more effectively. Higher order theories (TSDT and PSDT) provide consistent and realistic prediction of normal stresses and shear stresses. The results evaluated by higher theories confirm that higher order plate theories are essential for analysis under thermal loadings.

The variation of these displacements and stresses are shown in Figures 4-6. The variations of axial displacement, normal stress and shear stress across the thickness (h) evaluated by trigonometric shear deformation theory (TSDT) under linear and nonlinear thermal loadings is shown in Figures 4-6 respectively. The higher values of axial displacement and nonlinear variation of normal stress across thickness (h) is seen under nonlinear thermal load and shown in Figures 4 and 5. The transverse shear stresses evaluated by 3D equations of equilibrium are zero at upper and lower surfaces of plate under cylindrical bending. The nonlinear variation and realistic curve of shear stresses is seen across the thickness (h) of plate as shown in Figure 6. Table 2 shows negative stresses under nonlinear thermal loading which indicates that nonlinear thermal effects induce compressive type stresses in the plate undergoing cylindrical bending. On the other hand, CPT and FSDT yield zero stress prediction under same conditions. This shows their limitations in capturing nonlinear response.

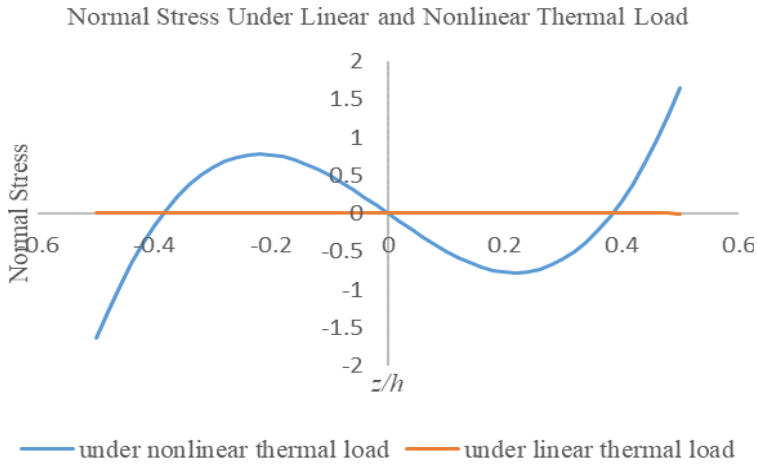

Figure 5. Variation of normal stress ($\bar{\sigma}_x$) across the thickness (h) under linear and nonlinear thermal load for an aspect ratio 4

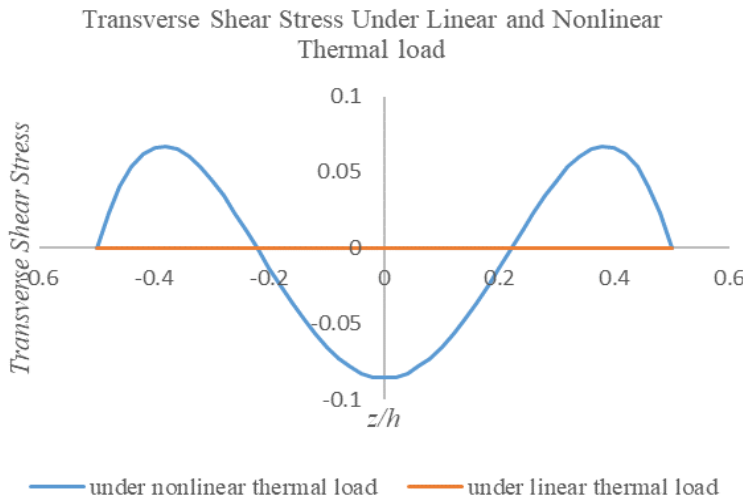

Figure 6. Variation of transverse shear stress ($\bar{\tau}_{zx}$) across the thickness (h) under linear and nonlinear thermal load for an aspect ratio 4

4. CONCLUSION

The study explores the thermal behaviour of an orthotropic laminated plate subjected to cylindrical bending under both linear and nonlinear thermal loading conditions, employing trigonometric shear deformation theory. The finding revels a pronounced increase in thermal displacements and stress levels when the thermal load transitions from a linear to nonlinear profile. This shift underscores the sensitivity of plate's structural response to the nature of thermal input.

Furthermore, under nonlinear thermal loading the results obtained using trigonometric shear deformation theory show only a slight deviation from those predicted by PSTD. This implies that both higher order theories are capable of capturing the intricate thermal effects with reasonable accuracy.

In real world applications, thermal loads are seldom uniform or linear. Nonlinear thermal loading reflects a more realistic and complex distribution of heat across the structure

which significantly influences the mechanical response. By incorporating these nonlinear effects, the analysis yields a more precise prediction of plate's behaviour.

Higher order theories, such as trigonometric and parabolic models are better equipped to account for these complexities. Their ability to represent the through thickness variation of temperature and shear strains make them especially valuable in evaluating the performance of laminated composite structures under thermal stress. The comparative results reinforce the importance of using advanced modelling approaches when dealing with nonlinear thermal environment as they provide deeper insights into the structural integrity and reliability of such systems. A key limitation of this study is the assumption of simply supported boundary conditions which may not fully represent the complexity of real-world structural constraints. One of key area for future studies is the integration of coupled thermo-mechanical effects were both temperature variation and mechanical forces acts on the laminates undergoing cylindrical bending. Another important area for future studies is the extension of this work and study of optimization. This will improve overall structural efficiency.

ACKNOWLEDGMENT

The author expresses sincere gratitude to Symbiosis Institute of Technology, Pune, for their unwavering support and motivation throughout the course of this work. Their consistent encouragement played a vital role in the successful completion of this study.

REFERENCES

[1] Sayyad, A.S., Ghumare, S.M., Sasane, S.T. (2014). Cylindrical bending of orthotropic plate strip based on nth-order plate theory. Journal of Materials and Engineering Structures, 1(2): 47-57.

[2] Sayyad, A.S., Ghugal, Y.M. (2016). Cylindrical bending of multi-layered composite laminates and sandwiches. Advances in Aircraft and Spacecraft Science, 3(2): 113-148. http://doi.org/10.12989/aas.2016.3.2.113

[3] Kant, T., Shiyekar, S.M. (2008). Cylindrical bending of piezoelectric laminates with a higher order shear and normal deformation theory. Computers and Structures 86(15-16): 1594-1603. https://doi.org/10.1016/j.compstruc.2008.01.002

[4] Pagano, N.J. (1969). Exact solution for composite laminates in cylindrical bending. Journal of Composite Materials 3(3): 398-411. https://doi.org/10.1177/002199836900300304

[5] Perel, V.Y., Palazotto, A.N. (2001). Finite element formulation for cylindrical bending of a transversely compressible sandwich plate based on assumed transverse strain. International Journal of Solids and Structures, 38(30-31): 5373-5409. https://doi.org/10.1016/S0020-7683(00)00293-6

[6] Khdeir, A.A. (2001). Free and forced vibration of antisymmetric angle ply laminated plate strips in cylindrical bending. Journal of Vibration and Control 7(6): 781-801. https://doi.org/10.1177/107754630100700602

[7] Kapuria, S., Kumari, P. (2011). Extended Kantorovich method for three-dimensional elasticity solution of laminated composite structures in cylindrical bending. Journal of Applied Mechanics 78(6): 1-8. https://doi.org/10.1115/1.4003779

[8] Kulkarni, S. (2024). A higher order computational model for thermal analysis of orthotropic plate in cylindrical bending. Civil and Environmental Engineering, 21(1): 1-9. https://doi.org/10.2478/cee-2025-0001

[9] Bhaskar, K., Varadan T.K., Ali, J.S.M. (1996). Thermo-elastic solutions for orthotropic and anisotropic composite laminates. Composites Part B: Engineering, 27(5): 415-420. https://doi.org/10.1016/1359-8368(96)00005-4

[10] Dhepe, S.N., Bambole, A.N., Ghugal, Y.M. (2024). An elasticity solution of FGM rectangular plate under cylindrical bending. Acta Mechanica, 235(1): 303-322. https://doi.org/10.1007/s00707-023-03758-1

[11] Milić P., Marinković D., Klinge S., Ćojbašić Ž. (2023). Reissner-mindlin based isogeometric finite element formulation for piezoelectric active laminated shells. Tehnicki Vjesnik, 30(2): 416-425. https://doi.org/10.17559/TV-20230128000280

[12] Khudoynazarov, K. (2024). Longitudinal-radial vibrations of a viscoelastic cylindrical three-layer structure. Facta Universitatis, Series: Mechanical Engineering, 21(4): 473-484. https://doi.org/10.22190/FUME231219010K

[13] Sayyad, A.S., Ghugal, Y.M. (2015). A n^{th} order shear deformation theory for composite laminates in cylindrical bending. Curved and Layered Structures, 2(1): 290-300. https://doi.org/10.1515/cls-2015-0016

[14] Dube, G.P., Upadhyay, M.M., Dumir, P.C., Kumar, S. (1998). Piezo-thermoelastic solution for angle ply laminated plate in cylindrical bending. Structural Engineering and Mechanics: An International Journal, 6(5): 529-542. https://doi.org/10.12989/sem.1998.6.5.529

[15] Garg, N., Prusty, B.P., Song, C., Phillips, A.W. (2020). Cylindrical bending of thick laminated composite plates using scaled boundary finite element method. Engineering Analysis with Boundary Elements, 120: 73-81. https://doi.org/10.1016/j.enganabound.2020.08.009

[16] Vel, S.S., Batra, R.C. (2001). Exact solution for cylindrical bending of laminated plates with embedded piezoelectric shear actuators. Smart Materials and Structures, 10(2): 240. https://doi.org/10.1088/0964-1726/10/2/309

[17] Vel, S.S., Batra, R.C. (2000). Cylindrical bending of laminated plates with distributed and segmented piezoelectric actuators/sensors. AIAA Journal, 38(5): 857-867. https://doi.org/10.2514/2.1040

[18] Heyliger, P., Brooks, S. (1996). Exact solutions for laminated piezoelectric plates in cylindrical bending. Journal of Applied Mechanics, 63(4): 903-910. https://doi.org/10.1115/1.2787245

[19] Kumar, A., Sahoo, S. (2021). Cylindrical bending analysis of laminated composite plates using higher order shear deformation theory and finite element method. Composite Structures, 256, 113058. https://doi.org/10.1016/j.compstruct.2020.113058

[20] Ostadzadeh, S.M., Baghestani, A.M., Afrasiab, H., Gholami, M. (2024). Quasi-static bending analysis of composite laminated cylindrical panels under hygrothermal conditions. Thin-Walled Structures, 203: 112227. https://doi.org/10.1016/j.tws.2024.112227

[21] Qian, H., Wang, Z., Lu, C., Cai, D. (2024). Thermal behaviors of composite laminated plates with arbitrary supports under non-uniform temperature boundary conditions. Thin-Walled Structures, 197: 111595. https://doi.org/10.1016/j.tws.2024.111595
[22] Huang, Z., Peng, L. (2021). Geometrically nonlinear bending analysis of laminated thin plates based on CLPT and deep energy method. Composite Structures, 262: 113353.
[23] Liu, T., Sun, X., Hu, W., Wang, L., Zhang, S., Bui, T.Q. (2024). Nonlinear thermal-mechanical coupled isogeometric analysis for GPL-reinforced functionally graded porous plates. Engineering Structures, 319: 118827. https://doi.org/10.1016/j.engstruct.2024.118827
[24] Liu, J., Zhou, Y., Meng, Y., Mei, H., Yue, Z., Liu, Y. (2025). Static and vibration analysis of imperfect thermoelastic laminated plates on a Winkler foundation. Materials, 18(15): 3514. https://doi.org/10.3390/ma18153514
[25] Zang, Q., Liu, J., Ye, W., Yang, F., Lin, G. (2023). A novel isogeometric scaled boundary finite element method for bending and free vibration analyses of laminated plates with rectilinear and curvilinear fibers constrained or free from elastic foundations. Engineering Analysis with Boundary Elements, 154: 197-222. https://doi.org/10.1016/j.enganabound.2023.05.040
[26] Ye, W., Zang, Q., Liu, J., Yang, F., Lin, G. (2023). Three-dimensional bending and free-vibration analyses of laminated cylindrical panels with/without elastic foundation using a two-dimensional discrete method. Soil Dynamics and Earthquake Engineering, 168: 107831. https://doi.org/10.1016/j.soildyn.2023.107831
[27] Zhou, Y., Liu, J., Mei, H., Hou, D., Yue, Z., Zhang, Y. (2025). Study on the effects of initial stress and imperfect interface on static and dynamic problems in thermoelastic laminated plates. Science and Engineering of Composite Materials, 32(1): 20240050. https://doi.org/10.1515/secm-2024-0050
[28] Liu, Z., Chen, X., Wang, W., Xiao, Y. (2024). Multi-objective optimization on thermomechanical behaviors of graphene nanoplatelet-reinforced sandwich plates. Chinese Journal of Aeronautics, 37(2): 103363.
[29] Kulkarni, S.K. (2025). A computational model for transverse thermal displacements in symmetric sandwich beam by using higher order shear deformation theory. Mathematical Modelling of Engineering Problems, 12(3): 917-924. https://doi.org/10.18280/mmep.120318

NOMENCLATURE

ε_x	normal strain
γ_{zx}	shear strain
E	modulus of elasticity
G	shear modulus
$\bar{u}$	normalized axial displacement
$\bar{w}$	normalized transverse
$\bar{\sigma}_x$	normalized normal stress
$\bar{\tau}_{zx}^{EE}$	normalized transverse shear stress obtained by using equilibrium equation
$[K]$	stiffness matrix
$(\bar{Q}_{ij})$	reduced stiffness coefficient
$\{f\}$	force vector
$\left[\frac{E_1}{E_2}\right]$	modular ratio
E_1	modulus of elasticity in fibre direction
E_2	modulus of elasticity in transverse direction
L	linear thermal load
NL	nonlinear thermal load
S	aspect ratio $\left(S = \frac{a}{h}\right)$
h	thickness of plate
a	length of plate along x axis
b	length of plate along y axis
Eq. (18)	$D_1 = Q_{11}\frac{h^3}{12},\ D_4 = Q_{11}(0.0645h^3)$
Eq. (19)	$D_9 = Q_{11}(0.0506h^3),\ D_{11} = Q_{55}(0.5\,h)$
Eq. (20)	$R_1 = \frac{h^2}{12}(\alpha_x Q_{11}), R_2 = \frac{2h^2}{\pi^3}(\alpha_x Q_{11})$
Eq. (21)	$R_5 = \frac{2h^2}{\pi^3}(\alpha_x Q_{11}), R_6 = \frac{h^2}{2\pi^2}(\alpha_x Q_{11})$

Greek symbols

$\left[\frac{\alpha_2}{\alpha_1}\right]$	ratio of coefficient of thermal expansion
α_2	coefficient of thermal expansion in transverse direction
α_1	coefficient of thermal expansion in fiber direction
θ	angle between fiber axis and reference axis x. In present case $\theta = 0$. Hence, $\alpha_1 = \alpha_x$ and $\alpha_2 = \alpha_y$
δ	variational operator
μ_{ij}	Poisson's ratio